Comparison between Michelson Interferometer and Fabry Perot Interferometer based on Silicon Photonics Technology

[a]Swati Shinde,[b]Riddhi Mudaliar,[c]Shraddha Nikam, [d]Rupesh Patil, [e]Foram Patel
Email id :[a]swati.shinde@somaiya.edu, [b]riddhi.mudaliar@somaiya.edu
[c]shraddha.nikam@somaiya.edu,[d]rupesh.lp@somaiya.edu ,[e]patel.fd@somaiya.edu

Abstract

Silicon photonics technology is a promising technology to build designs at low cost and in compact space. Optical fiber sensors play an important role because of benefits such as economy, adaptibility and compactness. We present michelson interferometer and fabry perot interferometer based on silicon photonics technology in small size and low loss which can be used in industrial applications and their results and comparison is shown.

1 Introduction

Silicon photonics is a technology that uses the common pattern in electronics of integrating large number of devices to increase performance and lower costs on photonic devices[1]. Silicon has a window of wavelength ranging from 1100 nm to 7000 nm approximately, which is far from being limited to the near-infrared (IR) communication band of 1300–1550 nm. It also has outstanding optical properties, like large optical damage threshold and thermal conductivity[2]. Silicon-on-insulator (SOI) has been the main material platform for silicon photonic waveguide components mainly because of its potential of high-integration density and compatibility with mature CMOS technologies[3]. It is extremely good for confining and manipulating light at the submicrometer scale and has the advantage of leveraging the enormous manufacturing infrastructure developed by the silicon microelectronics industry[4]. Michelson Interferometer is also used in sensors. When optical sensor is used within an integrated optics context, the advantages of optical sensing are significantly improved. Optical fibre sensors have become a vital part in development of sensors. The reasons include advantages of economy, adaptability, compactness and electromagnetic isolation compared with traditional electronic sensors[5].
For different sensing applications, different Integrated fiber Michelson Interferometers(IMIs) have been developed. IMIs are mostly based on modal interference in single fibers. Such kind of IMIs can be realized by different configurations such as tapers, long period grating, lateral-offset junction, and core mode fields mismatch. These modal interference based IMIs have advantages of low cost, easy fabrication, and high sensitivity[6]. Michelson interferometer modulator (MIM) is one of the schemes of folded modulators. With reflective mirrors on both arms, the interaction length between the light wave and modulating electrical field doubles. As a result, MIM can efficiently enhance modulation efficiency and/or

reduce device size[7].
One of the other interferometers are fabry perot interferometer.The working of fabry Perot interferometer is based on the principle of multiple beam interference[8].Fabry Perot interferometer can be used effectively in biological and chemical applications as many of the substances and bio-chemical reaction can be studied by the measurement of refractive index. Sensors based on FPI shows very high Refractive index sensitivity[9].FPI can also be used to for several other sensing applications such as temperature, strain, magnetic field and pressure because of its easy and design which can be fabricated easily. Although temperature plays an important role here in measurement of these physical properties[10].FPI sensors comes with advantage of simple structure design, high sensitivity, compact size. The most commonly used FPI sensors comprises of fibers having air cavities. This increases the fabrication cost. Shorter the length of air cavities, higher the sensitivity of FPI sensor[11].

2 Michelson Interferometer

Michelson Interferometer is the base stone of Time Domain Optical Coherence Tomography (OCT), in which the interference pattern generated by the reference arm and the sample arm produces sample density information in time, that is, the integration of the interference pattern power density in various position. one of the applications of wave superposition is michelson interferometer. Constructive or destructive interference can be detected when two waves are superposed. The amplitude of two superposed waves of same phase in michelson interferometer can be calculated as:

$$E_0{}^2 = E_{01}{}^2 + E_{02}{}^2 + 2E_{01}E_{02} \tag{1}$$

And the amplitude of waves have 180° different phase can be written as:

$$E_0{}^2 = E_{01}{}^2 + E_{02}{}^2 - 2E_{01}E_{02} \tag{2}$$

Sensitivity is displacement of optical path which causes the fringe pattern intensity to cycle from a maximum to a minimum. Michelson interferometer standard sensitivity is given as

$$S = \frac{\lambda}{2} \tag{3}$$

as λ is the wavelength of the laser being used. With multiple reflection sensitivity can be enhance to over $\frac{\lambda}{100}$. The sensitivity is based on the number of reflections as well as in the mirror assembly. There are few working to obtain high resolution in the two beam interferometer, like a multiple total internal reflection interferometer, which was used to measure the changes in the displacement in the order of micro to nano magnitude range[12]. Normal Michelson interferometer can measure object displacement with wavefront shapes to one half of the laser wavelength In Michelson interferometer, the minimum displacement that can be measured is$\frac{\lambda}{4}$. In the multiple reflection interferometer, the displacement sensitivity is given by:

$$D_m = \frac{\lambda}{4} * \frac{sin\theta}{sinN\theta} \tag{4}$$

where N gives the total number of reflections, λ is the wavelength of the laser in the system and θ is the angle of the two-mirror wedge. The common multiple reflection interferometer

is an improved version of the Michelson interferometer, due to increase in sensitivity its value for practical use also increased.[13].
The Michelson interferometer does not measure the infrared spectrum directly, but an 'interferogram' is measured, and is converted to a single-beam spectrum through fourier transformation. Due to this critical role of this transformation, the method is generally mentioned to as Fourier-transform infrared spectroscopy, or 'FT-IR'. Instruments referring to this design it has been recently proven to be fitted for a number of near-IR applications. A standard michelson interferometer has light passing through port 1 of 2 x 2 multimode interferometer which splits in two parts, where one part of the light goes to the mirror to get reflected and the other part of the light undergoes via phase shift to mirror to get reflected and get output at port 2[14]. Figure 1. shows the block diagram of michelson interferometer.

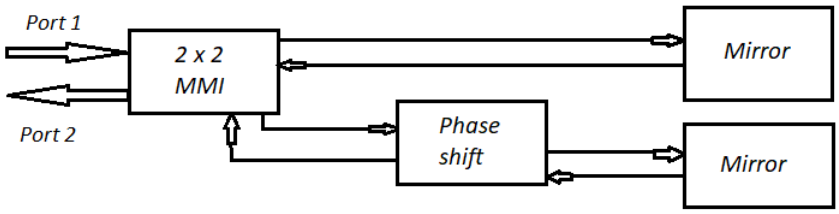

Figure 1. Block diagram of Michelson Interferometer.

$$\Delta\theta = \frac{2\pi\Delta\lambda}{FSR} \tag{5}$$

where $\Delta\ \lambda$ is the wavelength shift of the spectral notch FSR is free spectral range. The modulation efficiency, determined by the light-carrier overlap in the phase shifter, was characterized by the voltage-length product V_πxL_π. The V_πxL_π of the Michelson interferometer modulator was calculated by

$$V_\pi * L_\pi = \frac{V * FSR * L}{2 * \lambda} \tag{6}$$

where V is the applied voltage, FSR is the free spectral range determined by the michelson interferometer path length difference, L is the length of phase shifter and λ is the spectrum notch shift[15].

3 Fabry-parot interferometer

In fabry-parot The incident beam (I0) with the small incident angle (α) spreads into the optical cavity which is composed of the measurement and reference mirrors. Laser beams travel forwards and backward in optical cavity and are divided into many transmitted beams.For each transmitted beam the elecrtic field equation is given as:

$$ER = A0\sqrt{1-R}e^{i(wt+kx)} \tag{7}$$

Usually the Fabry–Pérot interferometers are devices with free-space light transmit between the mirrors.However,the term is sometimes also used for devices containing in a waveguide.[17] A high-resolution interferometer, the Fabry-Perot Interferometer has a resolvance of

$$\frac{\lambda}{\Delta\lambda} = \frac{m\pi\sqrt{r}}{1-r} \tag{8}$$

m=order of interference. r=reflectance of etalon surfaces. This means that least separation of two spectral lines is given by:

$$\lambda = \frac{m\Delta\pi\sqrt{r}}{1-r} \tag{9}$$

The spectral response of a Fabry-Pérot resonator is based on interference between the light launched into it and the light flow in the resonator. Constructive interference takes place if the two beams are in phase, leading to resonant enhancement of light inside the resonator. If the two beams are not in phase, only a tiny portion of the launched light is stored inside the resonator. That stored, transmitted, and reflected light is spectrally modified compared to the incident light. Intrinsic propagation losses inside the resonator can be quantified by an intensity-loss coefficient

$$1 - L_{\mathrm{RT}} = e^{-\alpha_{\mathrm{loss}} 2\ell} = e^{-t_{\mathrm{RT}}/\tau_{\mathrm{loss}}}. \tag{10}$$

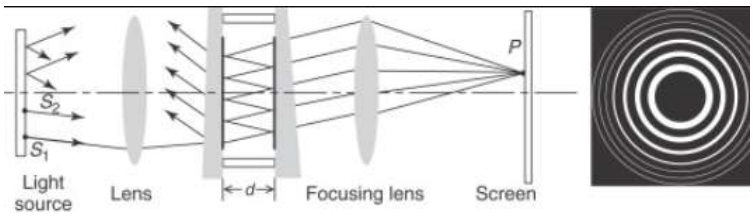

Figure 2. Block diagram of fabry perot interferometer

As seen in the figure the multiple beam interferometer which is also called as Fabry–Perot interferometer it consists of two plane parallel highly reflecting surfaces separated by distance d .Light coming in the volume between the mirrors can be partly reflected and transmitted by the surfaces.Light coming in the volume between the mirrors can be partly reflected and transmitted by the surfaces.The distance d generally ranges from several millimeters to several centimeters when the apparatus is used interferometrically, and to few tens of centimeters or more when it serves as a laser resonant cavity.Consider a point source S1 and one ray emitted, entering by way of the partially reflecting plate, it is multiply reflected within the gap. The transmitted rays are collected by a lens and brought to a screen. The multiple waves generated in the cavity, arriving at P from S1 are coherent among themselves. All the rays incident on the parallel plates at a given angle will result in a circular fringe of uniform irradiance. The interference bands will be narrow concentric rings, corresponding to multiple-beam transmission pattern. The phase difference between two successively transmitted waves is

$$\delta = \frac{4 * \pi * n}{\lambda_0} d\cos\theta_t + 2\psi \tag{11}$$

where ψ = additional phase shift introduced by metallic films at the surfaces d is so large and λ 0 so small that ψ can be neglected. Reflectance(R)= The fraction of the flux density

reflected at each incidence,T= the transmittance.We can neglect absorption from the metal films that are used to increase the reflectance, and consider R + T = 1. As a final comment on interferometers, it needs to be highlighted out that these days much of the progress in the field of interferometry has come not from inventing new forms of interferometers, but from powerful fringe analysis methods, such as phase-shift interferometer analysis in optical testing, mostly helped by computer data treatment, and also from making instruments that are user-friendly.

4 Results and Discussion

4.1 Michelson Interferometer

A 2D model of michelson interferometer was designed on COMSOL Multiphysics software. 3dB directional coupler was designed with bend radius having 3μm and multimode interferometer have dimensions of 1.5μm x 3.72μm in wavelength 1550nm. Electromagnetic waves, beam envelopes physics is used to get output of the design via frequency domain. Finite element method was used for boundary mode analysis to get results. Light enters from port 1 of 3dB directional coupler which splits in two parts which enter in 2 x 1 multimode interferometer which acts as a mirror to get reflection of the light to get output power at port 2 of 3dB directional coupler. Figure 3. shows the electric field propogation of michelson interferometer designed using silicon and silicon dioxide as materials for core and cladding respectively. Output power of 0.5Watt is received in port 2.

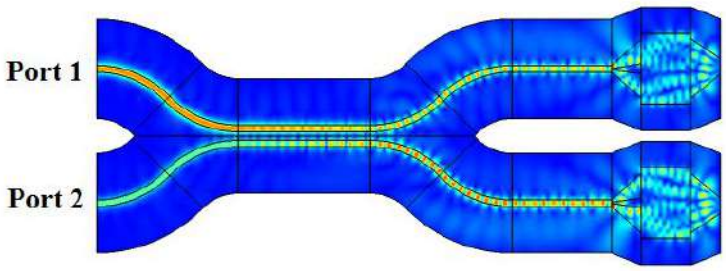

Figure 3. Electric field propogation in Michelson Interferometer

4.1.1 Bend Radius

The bend radius of 3dB directional coupler has been increased from 3μm to 10μm to check the effect on output power in port 2. Total modal transmission is observed by increasing the bend radius and also to note it's loss. Figure 4. shows the total modal transmission of 3dB directional coupler in michelson interferometer.

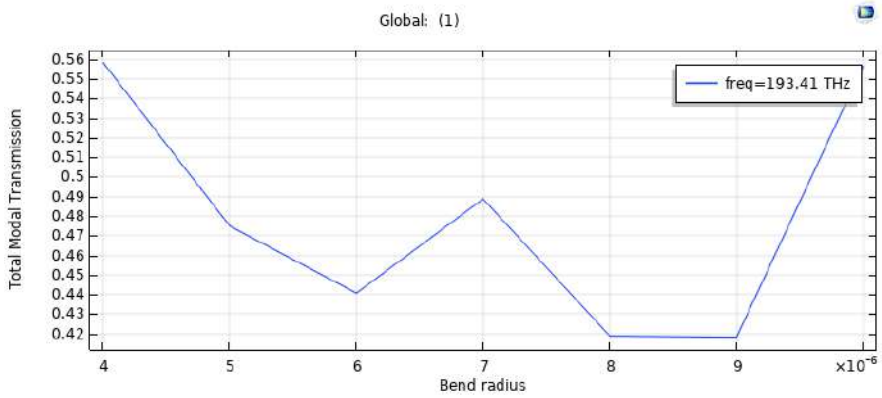

Figure 4. Total Modal Transmission in Michelson Interferometer

4.1.2 Length of directional coupler

The length of directional coupler is increased from 3μm to 10μm to note nature of power at port 2. The output power decreases with increase in length of directional coupler. Figure 5. shows the variation in output power due to change in length of directional coupler.

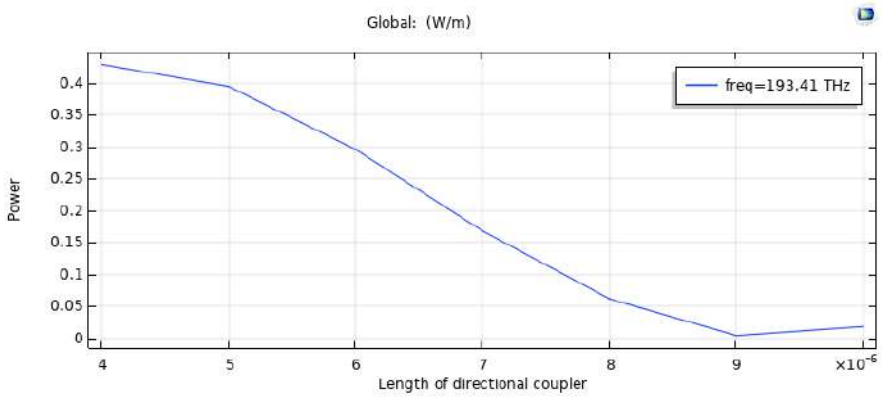

Figure 5. Change in power at port 2 due to increase in length of directional coupler in Michelson Interferometer

4.1.3 Length of Multimode Interferometer

Length of 2 x 1 multimode interferometer is increased from 1μm to 5μm to check the behaviour of power at port 2. The results show uncertainity in power at port 2. Figure 6. shows the graph of output power at port 2, when the length of 2 x 1 multimode interferometer is increased.

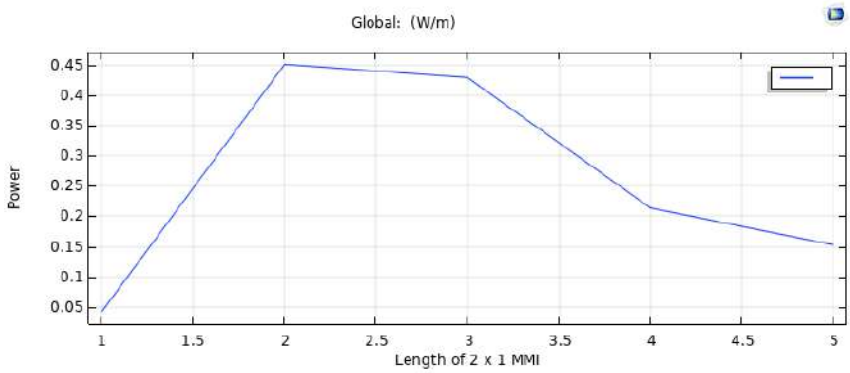

Figure 6. Change in power at port 2 due to increase in length of 2 x 1 Multimode Interferometer

4.1.4 S-Parameters

Scattering Parameters explain the electric field nature of the design.Table no.1 shows the values of s-parameters calculated for michelson interferometer in decibels.

Sr. No	S-parameters	dB
1.	S11	-4.9780
2.	S21	-18.659
3.	S31	-24.603
4.	S41	-11.878

4.1.5 Other Parametric Values

Sr. No	Parameters	Values
1.	Insertion Loss	-3.01dB
2.	Excess Loss	0
3.	Sensitivity	775nm
4.	Reflectance	0
5.	Transmittance	0
6.	Absorptance	1
7.	Wave Number	0.72 x 10^{-3}
8.	Electromagnetic Power loss Density	3.86 x 10^{-17} W/m
9.	Relative Permittivity Average	3.747 x 10^{-10} m^2

4.2 Fabry Perot Interferometer

COMSOL Multiphysics software was used to simulate fabry perot interferometer. Silicon and silicon dioxide material is used for the interferometer. Electromagnetic waves, frequency domain physics is used to get results of the model with the help of stuides such as eigenfrequency and frequency domain to observe the nature of the model. The dimensions of the model are 100nm x 10nm. Figure 7. shows the electric field propogation in fabry perot interferometer. The electric field is calculated at the freuqency of 400THz.

Figure 7. Electric field propogation in Fabry Perot Interferometer

In fabry perot interferometer, two outer perfectly matched layer absorbs without any reflection. There is perfect magnetic conductor so that output is mirror symmetric about these planes. Eigenfrequency study is used for this model to specify number of eigen frequencies to get a particular frequency range. Figure 8. shows the graph where Q factors were calculated for a set of frequencies. The study has been adjusted so that there are only physical modes, but the nophysical modes can come back which are the solutions to eigenfrequency in fabry perot interferometer. We can crosscheck by making sure that nophysical modes should be Q factor less than a half.

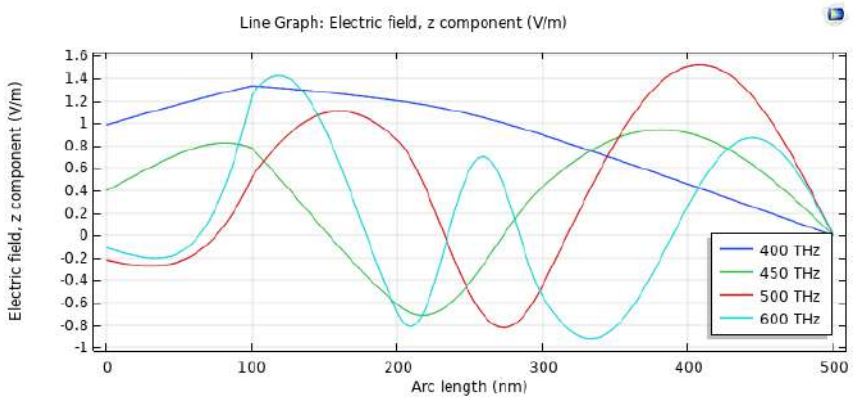

Figure 8. Electric field for Eigenfrequency problems in Fabry Perot Interferometer

The Q-factors for the frequencies are given below in table no. 2.

Sr. No	Frequencies	Q-Factor
1.	400THz	1.2057
2.	450THz	4.7773
3.	500THz	9.1528
4.	550THz	9.5921

For fabry perot interferometer, frequency domain was used to get electric field at 400THz and monitor total energy density. The peak is correspondant to resonant frequency and Q-factor. Figure 9. shows the graph of total energy density over the range of frequencies.

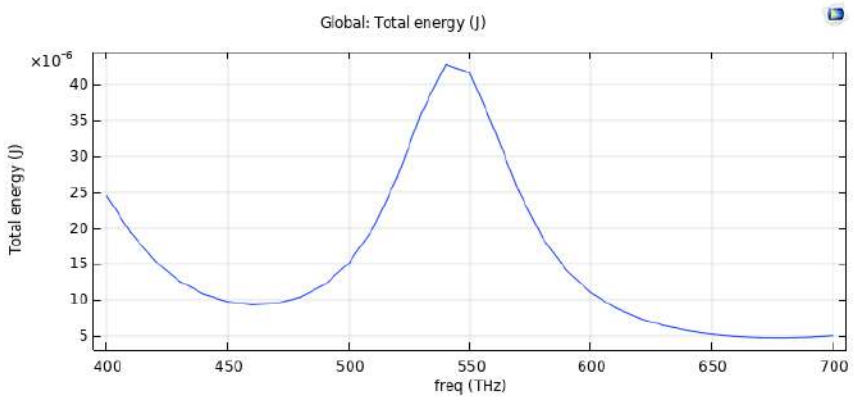

Figure 9. Total Energy Density over the range of frequencies in Fabry Perot Interferometer

5 Comparison

Table no. 3 shows the comparison between michelson interferometer(MI) and fabry perot interferometer(FPI)

Sr.No	Parameters	MI	FPI
1.	Dimensions	1.5μm x 3.72μm	100nm x 10nm
2.	Frequency	193.1THz	400THz
3.	Wave number	0.7203mm	8.38346 rad/m
4.	Total Electric Energy	1.576 x 10^{-13} J	1.2723 x 10^{-5} J
5.	Applications	Textile Yarn Industry Astronomy	Optical Equipments Spectroscopy
6.	Environmental Conditions	Unable to resist environmental disturbances	Able to resist environmental disturbances
7.	Advantages	Easy to setup, precise results can measure upto thickness of μm	simple optical design, suited to imaging system, high spectral resolving power
8.	Disadvantges	Hard to get precision Reflects 50% of light back to source	wavelength multiplexing is not possible, difficult to achieve high overall efficiency

6 Conclusion

In michelson interferometer , the effect of change in bend radius (varied from 3μm to 10μm) on output power appears to be non-linear and unpredictable. When the length of the directional coupler (varied from 3μm to 10μm) was varied we observed that the output power at the port 2 decreased gradually with the increase in the length of the directional coupler. The effect of change in the length of 2 x 1 multimode (varied from 1μm to 5μm) interferometer on the output power obtained at port 2 was uncertain. Increase in output power with the increase in length of 2 x 1 multimode interferometer was observed till certain point (2μm in our observation), then it decreased gradually with increase in length.
Where as in fabry perot interferometer, quality factor was calculated and with the help of eigenfrequency study, output at 400THz was able to achieve. In this paper, we proposed the design of michelson interferomter and fabry perot interferometer with silicon and silicon dioxide as a materials for core and cladding respectively. We obtained great results with

the use of these materials. Fabrication of products in photonic integrated circuits can be achieved with the merging of CMOS technology and silicon photonics technology. A photonic integrated circuit reduces heating of circuits significantly, ultimately increasing the performance and reducing the loss. The sensitivity is also achieved. The fabrication cost of devices such as sensors, modulators with these materials will get reduced.

References

[1]Xie, Min, Zhizhong Yuan, Bo Qian, and Lorenzo Pavesi. "Silicon nanocrystals to enable silicon photonics invited paper." Chinese Optics Letters 7, no. 4 (2009): 319-324.
[2]Zhou Fang, Ce Zhou Zhao, "Recent Progress in Silicon Photonics: A Review", International Scholarly Research Notices, vol. 2012, Article ID 428690, 27 pages, 2012. https://doi.org/10.5402/2012/428690
[3]Jalali, Bahram, and Sasan Fathpour. "Silicon photonics." Journal of lightwave technology 24, no. 12 (2006): 4600-4615.
[4]Pavel Cheben, Richard Soref, David Lockwood, Graham Reed, "Silicon Photonics", Advances in Optical Technologies, vol. 2008, Article ID 510937, 2 pages, 2008.
https://doi.org/10.1155/2008/510937
[5]Cao, Haoran, and Xuewen Shu. "Miniature all-fiber high temperature sensor based on Michelson interferometer formed with a novel core-mismatching fiber joint." IEEE Sensors Journal 17, no. 11 (2017): 3341-3345.
[6]Zhao, Yujia, Ai Zhou, Huiyong Guo, Zhou Zheng, Yimin Xu, Ciming Zhou, and Libo Yuan. "An integrated fiber michelson interferometer based on twin-core and side-hole fibers for multiparameter sensing." Journal of Lightwave Technology 36, no. 4 (2017): 993-997.
[7]Jian, Jian, Mengyue Xu, Liu Liu, Yannong Luo, Junwei Zhang, Lin Liu, Lidan Zhou, Hui Chen, Siyuan Yu, and Xinlun Cai. "High modulation efficiency lithium niobate Michelson interferometer modulator." Optics express 27, no. 13 (2019): 18731-18739.
[8]Yoshino, Toshihiko, Kiyoshi Kurosawa, Katsuji Itoh, and Teruzi Ose. "Fiber-optic Fabry-Perot interferometer and its sensor applications." IEEE Transactions on Microwave Theory and Techniques 30, no. 10 (1982): 1612-1621.
[9]Xu, Ben, Yi Yang, Zhenbao Jia, and D. N. Wang. "Hybrid Fabry-Perot interferometer for simultaneous liquid refractive index and temperature measurement." Optics express 25, no. 13 (2017): 14483-14493.
[10]Wu, Yongfeng, Yundong Zhang, Jing Wu, and Ping Yuan. "Temperature-insensitive fiber optic Fabry-Perot interferometer based on special air cavity for transverse load and strain measurements." Optics express 25, no. 8 (2017): 9443-9448.
[11]Tian, J., Jiao, Y., Fu, Q., Ji, S., Li, Z., Quan, M. and Yao, Y., 2018. A Fabry–Perot interferometer strain sensor based on concave-core photonic crystal fiber. Journal of Lightwave Technology, 36(10), pp.1952-1958.
[12] Wang, Minjuan, Linjie Zhou, Haike Zhu, Yanyang Zhou, Yiming Zhong, and Jianping Chen. "Low-loss high-extinction-ratio single-drive push-pull silicon Michelson interferometric modulator." Chinese Optics Letters 15, no. 4 (2017): 042501.
[13] Youn, Woonghee. "Increasing the Sensitivity of the Michelson Interferometer through Multiple Reflection." (2015).
[14]Li, Xianyao, Xi Xiao, Hao Xu, Zhiyong Li, Tao Chu, Jinzhong Yu, and Yude Yu. "Highly efficient silicon Michelson interferometer modulators." IEEE Photonics Technology Letters

25, no. 5 (2013): 407-409.
[15]Adams, Freddy, Silvio Aime, Laura A. Andersson, Isao Ando, David M. Andrenyak, David L. Andrews, Lester Andrews et al. "Encyclopedia of Spectroscopy and Spectrometry." (2010).
[16]ensors (Basel). 2010; 10(4): 2577–2586. Published online 2010 Mar 24. doi: 10.3390/s100402577